J Solid State Electrochem (2011) 15:1253–1261
DOI 10.1007/s10008-010-1185-7

ORIGINAL PAPER

Electrochemical behaviors of GMP based on solid-phase extractionon at Cu-Mg-Al hydrotalcite-like compound (HTLC) modified glass carbon electrode

Lin Cui · Lifang Li · Shiyun Ai · Huanshun Yin · Peng Ju · Tao Liu

Received: 19 May 2010 / Revised: 26 August 2010 / Accepted: 30 August 2010 / Published online: 19 September 2010

Abstract Guanosine-5′-monophosphate (GMP) was investigated the electrochemical behaviors based on solid-phase extractionon (SPE) at Cu-Mg-Al hydrotalcite-like compound (HTLC) modified glass carbon electrode. Cu-Mg-Al hydrotalcite-like compound (HTLC) was proved as a new sorbent for SPE of GMP, which showed an irreversible adsorption oxidation process on the HTLC/GCE with the oxidation peak potential located at 1.15 V (vs. SCE) in a pH 5.0 acetate buffer solution. Influencing factors of the electrochemical behavior of GMP on the HLTC/GCE were optimized and kinetic parameters were calculated. Under the optimal conditions, with differential pulse voltammetry (DPV), a linear relationship was obtained between the oxidation peak current and the GMP concentration in the range from 1.0×10^{-6} to 8.0×10^{-4} molL^{-1} with the detection limit as 5.0×10^{-7} molL^{-1} (signal-to-noise ratio of 3). The modified electrode surface has very good reproducibility and stability.

Keywords Guanosine-5′-monophosphate · Hydrotalcite-like compounds · Solid-phase extractionon · Electrochemistry

Introduction

Purine nucleotides play an important role in various biological processes. As one of them, guanosine-5′-monophosphate (GMP) can exert trophic effects on neural cells [1, 2], protect brain slices in a model of hypoxia [3], stimulate the removal of extracellular glutamate by astrocytes [4, 5] and protect against seizures induced by the glutamatergic agents, quinolinic acid (QA) or a-dendrotoxin (a-DTX) in rodents [6–9]. So, it is important to establish a sensitive method for the detection of GMP. Up to now, different analytical methods have been developed for the determination of GMP, based on thin layer chromatography [10], ion-pair HPLC [11] and high performance liquid chromatography (HPLC) [12]. Electrochemical methods can also be used for having the advantages of fast response, cheap instrument, low cost, simple operation, time saving, high sensitivity, excellent selectivity and real-time detection in situ condition. However, direct detection of GMP using electrochemical sensor is rare, because the response of GMP at traditional electrochemical sensor is poor. Therefore, different kinds of chemical modified electrodes were devised for GMP detection. Rajendra N. G. et al. investigated the electro-oxidation of guanosine-5′-triphosphate (GTP) at the pyrolytic graphite electrode [13] and gold nanoparticles modified indium tin oxide electrode [14]. Xie et al. [15] studied the electrochemical behavior of GMP at redox polymer film modified indium tin oxide (ITO) electrode. These works all showed the modified electrodes can facilitate its application to study the electrochemical behavior of GMP and its determination.

As new nano-composite materials, hydrotalcite-like compounds (HTLCs) have been received considerable attention in recent years. The layered structure consists metal cations that at least two different oxidation states with positive charges, and metal hydroxide layers separated from each other by anions and water molecules. The chemical composition of hydrotalcite-like compounds can be represented by $[M_{1-x}^{II}M_x^{III}(OH)_2]^{x+}[A_{x/n}{}^{n-}\ yH_2O]^{x-}$, where M^{II} and M^{III} represent divalent and trivalent metal ions within

L. Cui · L. Li · S. Ai (✉) · H. Yin · P. Ju · T. Liu
College of Chemistry and Material Science,
Shandong Agricultural University,
Taian,
271018 Shandong, People's Republic of China
e-mail: ashy@sdau.edu.cn

the brucite-like layers (Mg^{2+}, Zn^{2+}, Ni^{2+}, Co^{2+}, Cu^{2+}, Al^{3+}, Cr^{3+}, Fe^{3+}, Mn^{3+}, etc.), and A^{n-} is an *n*-valent anion (Cl^-, NO_3^-, ClO_4^-, CO_3^{2-}, SO_4^{2-}) [16, 17]. HTLCs are interested as electrode surface modifiers for the properties of the layered structures, large surface areas and anion exchange [18–20]. They are often used as catalysts or catalyst precursors, ion exchangers, adsorbents, polymer stabilizers, etc. The copper-containing hydrotalcite-like compound can be used as a catalyst for the Baeyer-Villiger oxidation of ketones [21], the coupling of phenylethyne [22], alkylation of phenol [23] and removal of nitrogen oxides [24]. So far, hydrotalcite-like compounds (HTLCs) present excellent catalytic properties and intense adsorbability for a number of processings of technological interest, and these nanocomposites can prevent biomolecules from degradation and the functionalized HTLCs can facilitate the electron transfer between protein and electrode [25].

In this paper, SPE as the most popular sample preparation method of GMP to Cu-Mg-Al hydrotalcite-like compound (Cu-Mg-Al HTLC) serving as sorbent was investigated. The oxidation response of GMP indicated that HTLC could present excellent extraction behaviors. The purpose of the present work is to construct a stable, sensitive and selective analytical method to determine GMP in a simple, fast, and inexpensive way. Based on the electrochemical response of GMP, a new electrochemical method for GMP detection was established and new electrochemical sensors with HTLCs would be developed.

Experimental

Reagents and apparatus

Guanine, guanosine and guanosine-5′-monophosphate (GMP) were purchased from Pure Crystal Reagent Ltd. (Shanghai) and used as received. Acetate buffer solutions were prepared by mixing stock solutions of 0.2 $molL^{-1}$ CH_3COOH and 0.2 $molL^{-1}$ CH_3COONa and adjusting the pH with 0.2 $molL^{-1}$ CH_3COOH or 0.2 $molL^{-1}$ NaOH. Other chemicals were of analytical reagent grade and all the solutions were prepared with redistilled deionized water.

Electrochemical experiments were performed with CHI 660C electrochemical workstation (Shanghai Chenhua Co., China) with a conventional three-electrode cell. The working electrode is a bare glass carbon electrode (d= 2 mm) or modified glass carbon electrode. A saturated calomel electrode (SCE) and a platinum wire were used as reference electrode and auxiliary electrode, respectively. Fourier transform infrared (FT-IR) spectra was recorded with a Perkin-Elmer Model 1750 spectrometer (USA). Powder X-ray diffraction patterns were recorded using a Rigaku D/MAX 2200PC X-ray diffractometer (Japan) with Cu K_α radiation (λ =0.154178 nm, graphite monochromator, 28 kV and 20 mA), a 2θ range from 8° to 80° was investigated at a scanning speed of 10° min^{-1}. Scanning electron microscopy (SEM) was performed on a Hitachi S-3000N instrument (Japan).

Preparation of HTLC

The Cu-Mg-Al HTLC was prepared by titration of a mixture solution of mentallic ions with NaOH [26]. In brief, 20 mL solution containing 1.208 g of $Cu(NO_3)_2$, 3.846 g $Mg(NO_3)_2$ and 3.751 g $Al(NO_3)_3$ was titrated with 20 mL mixture solution of 2.40 g NaOH and 5.30 g Na_2CO_3 under vigorous stirring. During the synthesis, the temperature was maintained at 25°C. The resulting suspension was then maintained at 65°C with stirring for 1 h. The product was filtered off and washed thoroughly with deionized water until a neutral pH was observed, then dried at 80°C for 2 days in air. The resulted final white product was characterized with FT-IR, XRD and SEM.

Preparation of HTLC/GCE

Before modification, the bare GCE with a diameter of 3 mm was polished to mirror with 0.3 and 0.05 μm alumina slurry on micro-cloth pads, and rinsed thoroughly with redistilled deionized water, then washed successively with anhydrous alcohol and redistilled deionized water in an ultrasonic bath, respectively. Finally, it was dried in air before use. For preparation of modified electrode, 2 mg mL^{-1} HTLC solution was first prepared by dispersing HTLC in redistilled deionized water, and following ultrasonication for 1 h. With a microinjector, 10 μL of HTLC solution was dropped on the surface of GCE to obtain HTLC/GCE. The HTLC/GCE was stored at 4°C in a refrigerator when it was not in use. The same cleaned procedure was applied to the used electrode before the electrode was modified every time.

Results and discussion

Characterization of HTLC

The FT-IR spectra of HTLC showed in Fig. 1a. The intense broad band at 3466.56 cm^{-1} and the weak absorption band at 1633 cm^{-1} corresponded to the OH mode, caused by the interlayer water molecules and hydroxyl groups in the brucite-like layers [27, 28]. IR absorptions due to the v_2, v_3 and v_4 stretching vibration of interlayer CO_3^{2-} ions were recorded at around 651, 865 and 1369 cm^{-1}. This almost can be observed for every hydroxide irrespective to the nature of the octahedral sheets, suggesting a rather symmetric envi-

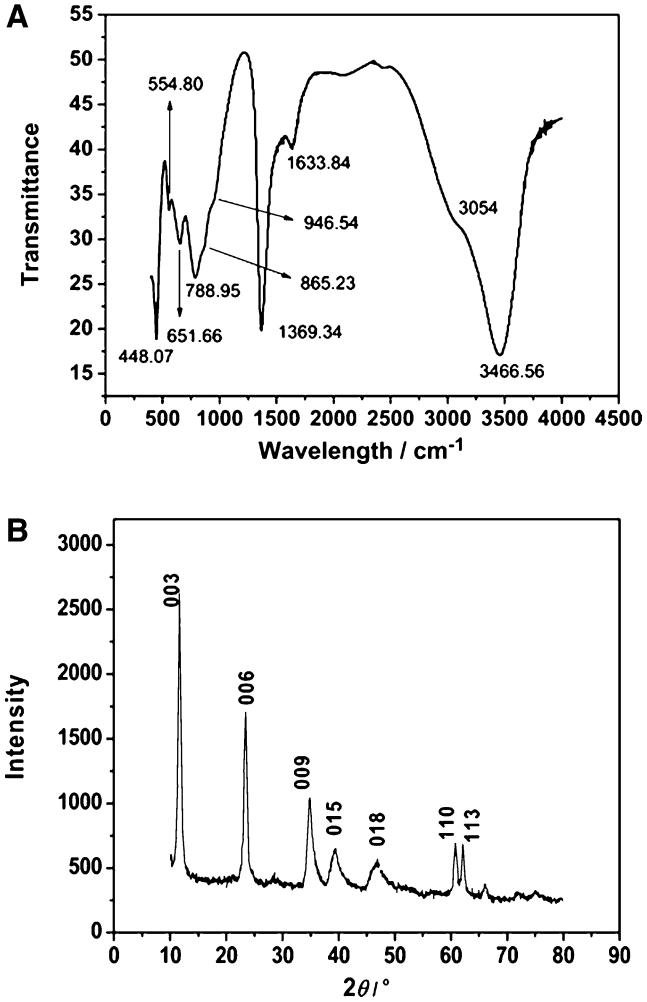

Fig. 1 FT-IR spectra **a** and Power XRD patterns **b** of Cu-Mg-Al HTLC

ronment for the interlayer anions [29]. The formation of the HTLC is confirmed with the peaks of 448, 554 and 788 cm^{-1}, which could be attributed to the presence of Mg-O, Al-O, Cu-O and O-M-O bands. Moreover, the result indicated the Cu-Mg-Al HTLC was successfully synthesized.

Figure 1b displayed the XRD diffraction pattern of Cu-Mg-Al HTLC. The sample was scaned for 2θ ranging from 10 to 80° due to CuO phase and its reflection at 35.71°, 38.96°, 48.05°, 38.89° [30]. The broad has less intense peaks at higher angles (peaks close to 2θ=38° and 46° ascribed to diffraction by (015) and (018) planes). The doublet close to 61° (2θ) corresponds to diffraction by plane (110) [31]. The results obtained in this work are in accordance with previous reports [32, 33] and the results of XRD can be concluded that Cu^{2+} was entered HTLC.

Surface morphology of HTLC/GCE

The SEM images of glassy carbon electrode coated by HTLC were shown in Fig. 2. The layer of irregularly flakes

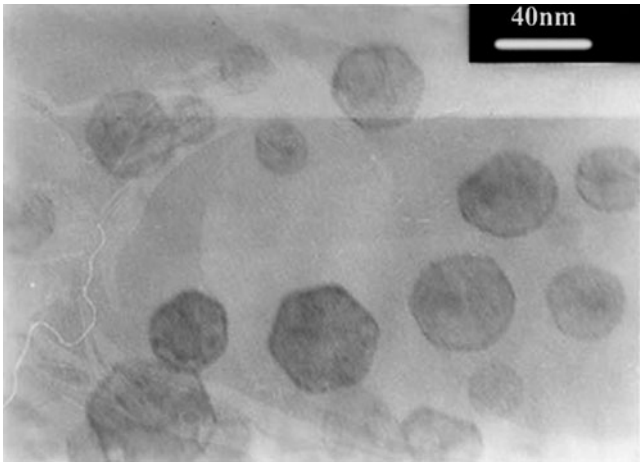

Fig. 2 SEM image of the surface of HTLC modified electrode

of HTLC was present and isolated with each other. It showed that the LDH prepared by the precipitation method directly was nano-scaled and three-dimensional with a size of 20–40 nm. It also demonstrated that the surface of HTLC/GCE was porous and rugged, which may allow the free entry of GMP into the inner layers, and could increase utilization of the whole film.

Characterization of electrochemical behavior of HTLC/GCE

Cyclic voltammograms of 5×10^{-3} $molL^{-1}$ $Fe(CN)_6^{3-/4-}$ at GCE (a) and HTLC/GCE (b) are shown in Fig. 3a. A couple of well-defined redox peaks were observed at bare GCE with peak-to-peak separation (ΔE_p) of 105 mV. But when the electrode was coated with HTLC, an increase in ΔE_p and a decrease in peak current (I_p) were observed. It proved that $[Fe(CN)_6]^{3-/4-}$ anions could incorporate into hydrotalcite-like compounds film, via long range electrostatic interactions with positively charge compounds surface, which could slow the rate of the electron transfer by switching from an aqueous to a clay phase [34, 35]. That is to say, the HTLC film itself introduced a resistance between electrode surface and $Fe(CN)_6^{3-/4-}$ into the electrode/solution system for its non-conductibility.

Electrochemical impedance spectroscopy (EIS) was carried out to probe the interfacial electron-transfer resistance (R_{et}) that aroused from every surface modification step. Generally, the semicircle portion observed at high frequencies in the Nyquist diagrams corresponds to the electron-transfer limiting process. The R_{et} value can be directly measured as the semicircle diameter [36]. The Nyquist diagrams of bare GCE (a) and HTLC/GCE (b) in 5.0×10^{-3} $molL^{-1}$ $[Fe(CN)_6]^{3-/4-}$ containing 0.1 $molL^{-1}$ KCl were shown in Fig. 3b. A smaller well defined semicircle at higher frequencies was obtained at the bare

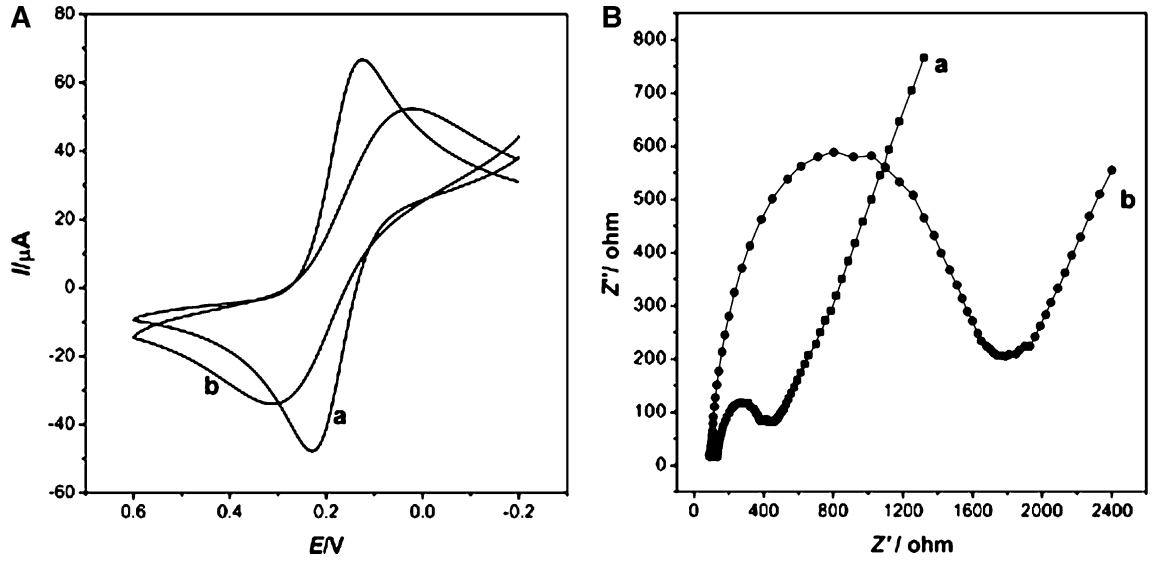

Fig. 3 Cyclic voltammograms **a** and Nyquist plots **b** of 5×10^{-3} molL^{-1} $Fe(CN)_6^{3-/4-}$ (1:1) in 0.1 molL^{-1} KCl solution recorded at GCE (*a*) and HTLC/GCE (*b*) Scan rate: 100 mVs^{-1}. The frequency range was from 0.1 to 10^5 Hz at the formal potential of 0.18 V

electrode than modified electrode, and this result indicated smaller interface impedance the bare GCE had comparing with the modified electrode. The experiment suggested HTLC was successfully immobilized on the GCE surface and would decrease the rate of electron transfer of $Fe(CN)_6^{3-/4-}$.

Cyclic voltammetric behaviors of GMP

Figure 4 showed cyclic voltammograms of GCE (a, d) and HTLC/GCE (b, c) in the presence (a, c) and absence (b, d) of 2×10^{-4} molL^{-1} GMP at scan rate of 100 mVs^{-1}.

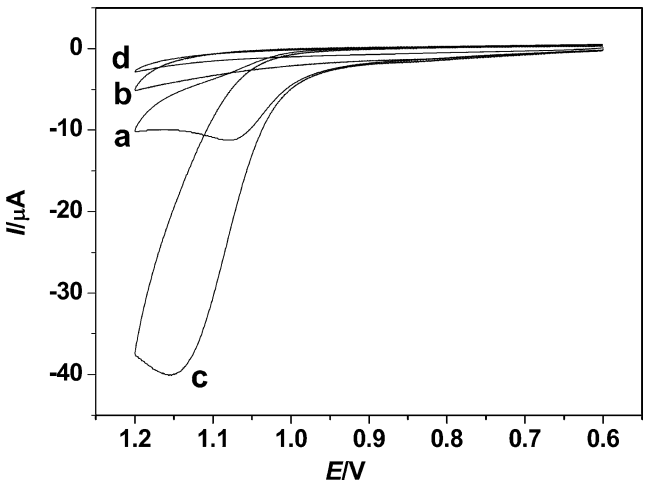

Fig. 4 Cyclic voltammograms of GCE **a**, **d** and HTLC/GCE **b**, **c** in the absence **b**, **d** and presence **a**, **c** of 2×10^{-4} molL^{-1} GMP in 0.2 mol L^{-1} acetate buffer solution (pH 5.0). Scan rate: 100 mV/s. Extraction time: 180 s. Extraction potential: +0.4 V

No redox peak was observed at GCE without GMP. The same phenomenon was also obtained at HTLC/GCE. From this, it can be concluded that HTLC is electro-inactive in the selected potential region. The oxidation peak potential of GMP at HTLC/GCE was increased than the bare electrode due to its non-conductibility. However, the oxidation peak current on the HTLC/GCE was about 4 times higher than the bare GCE in 2×10^{-4} molL^{-1} GMP after extraction. Moreover, no corresponding reduction peak of GMP was observed at both electrodes, indicating that the oxidation reaction was totally irreversible. Due to the adsorption of HTLC, more GMP could be extracted on the surface of HTLC modified electrode.

Optimization parameters

Optimization of experimental conditions for SPE and CV analysis

Since HTLC was the sorbent for SPE of GMP, its mount plays a key role on the detection response. The influence of HTLC load ranging from 0.5 to 4 mgmL^{-1} on the cyclic voltammetry of 2×10^{-4} molL^{-1} GMP in 0.2 molL^{-1} pH 5.0 acetate buffer solution was studied. As can be seen in Fig. 5a, the current response increased with increasing load amount of HTLC until it was 2 mgmL^{-1}, then decreased when HTLC load amount increased further, which might be caused by increasing film thickness. Hence, a HTLC load of 2 mgmL^{-1} was used throughout this work.

The influence of the pH value on the electrochemical response of GMP was investigated in the pH ranging from 3.6 to 5.6 with the results shown in Fig. 5b. The maximum

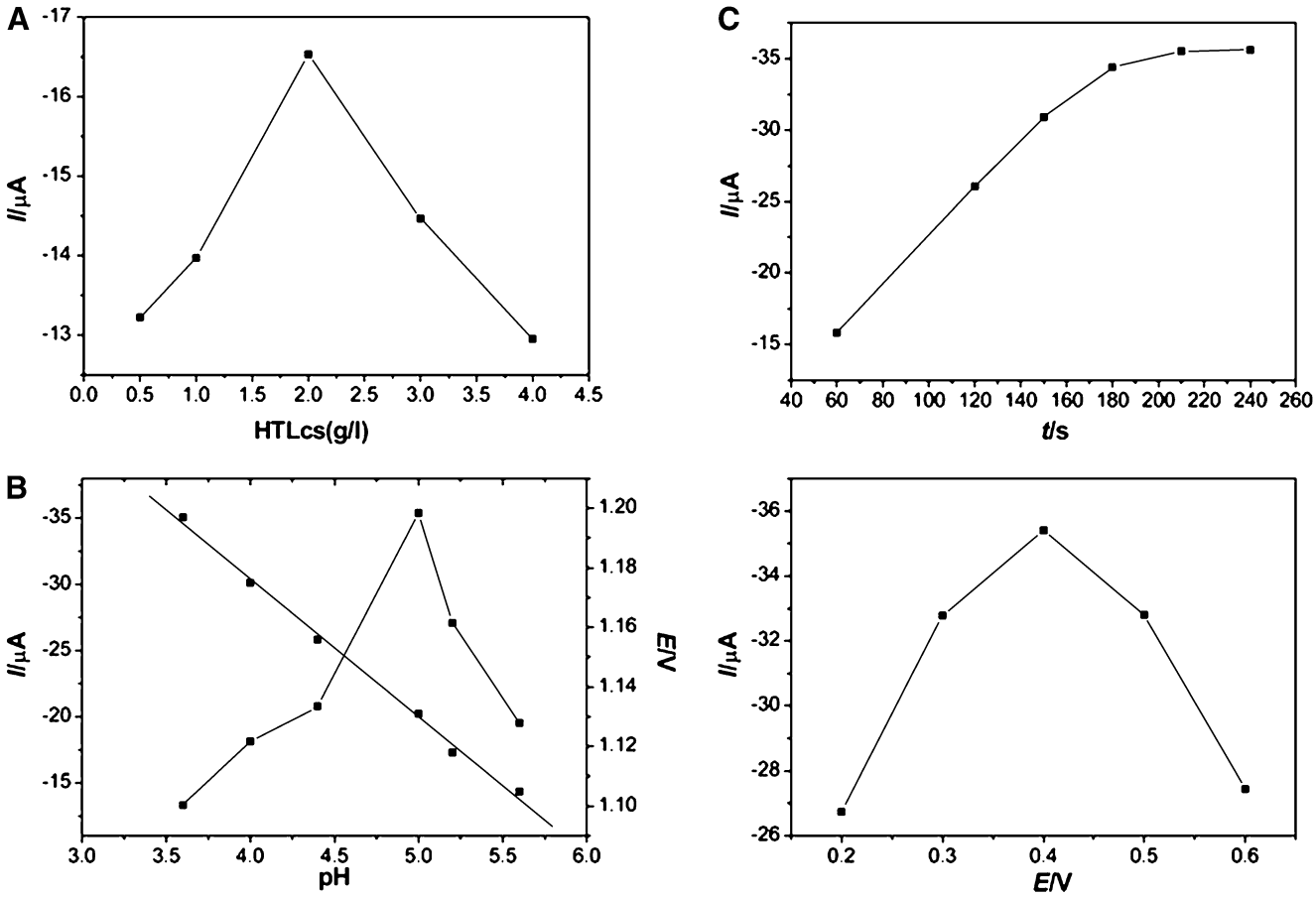

Fig. 5 **a** Dependence of current response for 2×10^{-4} molL^{-1} GMP oxidation on the content of HTLC, **b** Influence of buffer pH on the current (*a*) and potential (*b*) response of 2×10^{-4} molL^{-1} GMP at scan rate of 100 mVs^{-1}, **c** Effects of extraction time (*a*) and extraction potential (*b*) on the oxidation peak current of 2×10^{-4} molL^{-1} GMP

value of the oxidation peak current was obtained at pH 5.0. Considering the sensitivity of the determination of GMP, pH 5.0 buffer solution was selected for subsequent detection. As can be seen in Fig. 5b, the oxidation peak potential shifted to negative direction (straight line b) with increasing buffer pH, which indicated protons took part in the electrode reaction. The dependence of the oxidation peak potential of GMP with the buffer pH constructed with a linear regression equation as $E_{pa}(V) = -0.044pH + 1.3517(R = 0.9948)$.

The effect of extraction time for 2×10^{-4} molL^{-1} GMP at HTLC/GCE was investigated and the results were shown in Fig. 5c (a). It revealed that the oxidation peak current increased gradually as the extraction time up to 180 s and then leveled off. This phenomenon could be attributed to saturated adsorption of GMP on the modified electrode surface. So 180 s was chosen as the optimal extraction time. Meanwhile, Fig. 5c (b) showed the effect of extraction potential on oxidation peak current of 2×10^{-4} molL^{-1} GMP. When the extraction potentials shifted from +0.2 to +0.6 V, the maximum oxidation peak current was got at +0.4 V. So the extraction potential of +0.4 V was used for GMP detection.

Influence of scan rate

The influence of potential scan rate on the electrochemical responses of GMP in pH 5.0 acetate buffer solution was studied by cyclic voltammetry and the results were shown in Fig. 6a. With the increase of scan rate, the oxidation peak currents increased gradually. The inset of Fig. 6a showed the peak current increased linearly with the scan rate in the range from 20 to 100 mVs^{-1} and the linear regression equation was calculated as $I(\mu A) = -0.2180v(mVs^{-1}) - 9.014, (R = 0.9828)$. The result indicated that electrode process was controlled by adsorption, and the scan rate (100 mVs^{-1}) was employed for the whole experiment.

From Fig. 6b, it can be seen that E_{pa} changed linearly versus lnν with a linear regression equation of $E_{pa} = 0.02369\ln\nu + 1.0617(V, mVs^{-1}, R = 0.9940)$ in the range from 20 to 100 mVs^{-1}. For an adsorption-controlled and

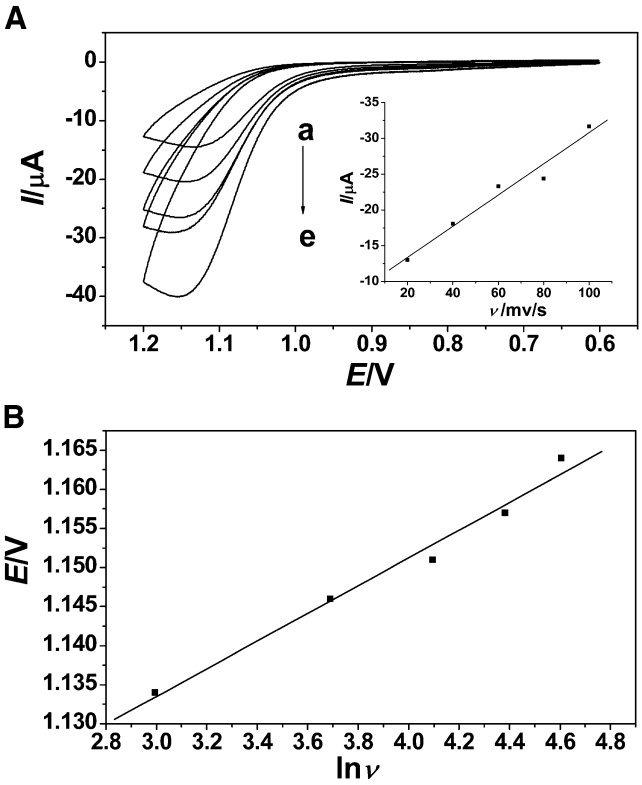

Fig. 6 **a** Cyclic voltammograms of 2×10^{-4} molL^{-1} GMP at HTLC/GCE in acetate buffer solution with different scan rates (from a to e: 20, 40, 60, 80, and 100 mVs^{-1}). Inset: the plot of peak current vs. scan rate. **b** The relationship between E_{pa} and lnν

irreversible electrode process, on the basis of Laviron method [37], E_{pa} is defined by the following equation:

$$E_{pa} = E^o + (RT/\alpha nF)\ln(RTk^0/\alpha nF) + (RT/\alpha nF)\ln\nu \quad (1)$$

where α is the charge transfer coefficient, k^0 is standard rate constant of the reaction, n is electron transfer number involved in the rate-determining step, ν is scan rate, and E^0 is formal potential. Other symbols have their usual meanings. Thus, the value of αn can be easily calculated from the slope of E_{pa}–lnν, the calculation value of αn is 1.08 (T=298, R=8.314, and F=96480). Generally, α is assumed to be 0.5 in totally irreversible electrode process. So, the value of the number of electron (n) was calculated to be 2. Integrating the result obtained in Optimization of experimental conditions for SPE and CV analysis and this Section, it can be concluded that the electrooxidation of GMP on HTLC/GCE is a two-electron and two-proton process. Therefore, the electrochemical oxidation mechanism of GMP on the HTLC may be expressed with the following equation: (Scheme 1).

The primary electrooxidation step including two steps of two-electron and two proton process with the free radical form involved an oxidation at N_7=N_8 position to give an 8-hydroxyguanosine-5′-monophosphate, which could be further oxidized to an unstable dimer with the above chemical reaction step. GMP has the same mechanism with guanosine, because they are oxidized the same part. The mechanism of the overall reaction can be described as oxidation, followed by deprotonation, another oxidation and deprotontional process, and the final coupling [38, 39]. The oxidation reaction of GMP was totally irreversible, therefore, no further oxidation peak was observed at the electrode surface.

Electrochemical parameter of electrode reaction

Electrochemical effective surface area A

Figure 7 showed the plots of Q-t and Q-$t^{1/2}$ at bare GCE and modified electrode in 1×10^{-4} molL^{-1} $K_3[Fe(CN)_6]$ containing 1 molL^{-1} KCl. From the slope of the plot of Q versus $t^{1/2}$ the electrochemical effective surface area for bare GCE and HTLC/GCE can be calculated by chronocoulometry using 1×10^{-4} molL^{-1} $K_3[Fe(CN)_6]$ as model complex (the diffusion coefficient D of $K_3[Fe(CN)_6]$ is 7.6×10^{-6} cm^{2}s^{-1} [40]) based on the Eq. 2 given by Anson [41]:

$$Q(t) = \frac{2nFAcD^{1/2}t^{1/2}}{\pi^{1/2}} + Q_{dl} + Q_{ads} \quad (2)$$

where n is electron transfer number, A is the surface area of the working electrode, c is the concentration of

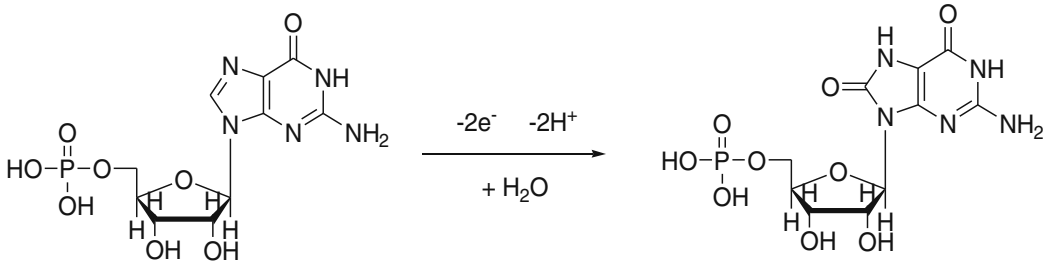

Scheme 1 The proposed electrooxidation mechanism of GMP

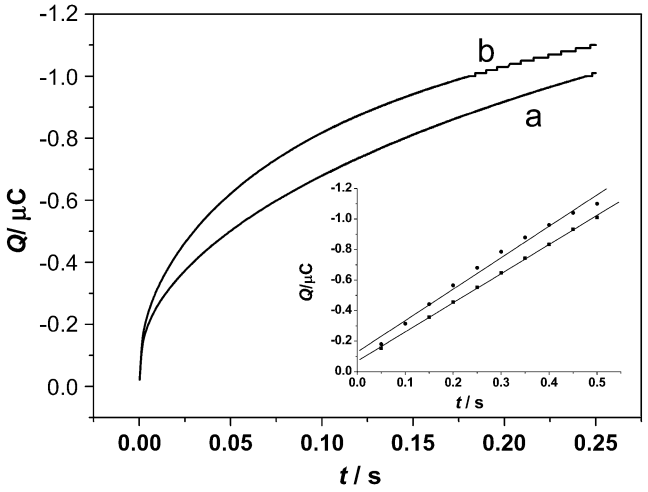

Fig. 7 Plot of Q-t curve of GCE **a** and HTLC/GCE **b** in 1×10^{-4} mol L^{-1} $K_3[Fe(CN)_6]$ containing 1 molL^{-1} KCl. Insert: plot of Q-$t^{1/2}$ curve on GCE **c** and HTLC/GCE **d**

substrate, D is the diffusion coefficient, Q_{dl} is double layer charge which could be eliminated by background subtraction, Q_{ads} is adsorption charge. Based on the slope of the linear relationship between Q and $t^{1/2}$, A can be calculated to be 0.03168 cm^2 and 0.03895 cm^2 for GCE (Fig. 7c) and HTLC/GCE (Fig. 7d), respectively. The results indicated that the electrode effective surface area was increased after modification of GCE with HTLC.

Differential electrochemical behavior of guanine, guanosine and GMP on the HTLC/GCE

The same concentration of 2×10^{-4} molL^{-1} of guanine, guanosine and GMP with HTLC modified electrodes were

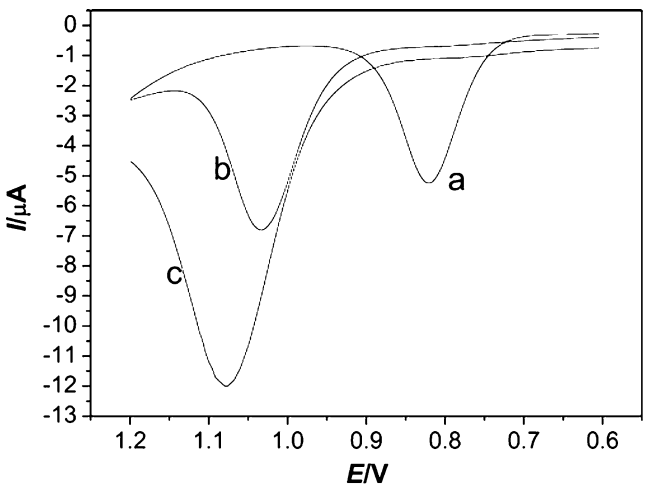

Fig. 8 Differential Pulse Voltammetry at HTLC/GCE in acetate buffer solution for concentration of 2×10^{-4} molL^{-1} of guanine **a**, guanosine **b**, GMP **c** in acetate buffer solution, scan rate: 100 mVs^{-1}

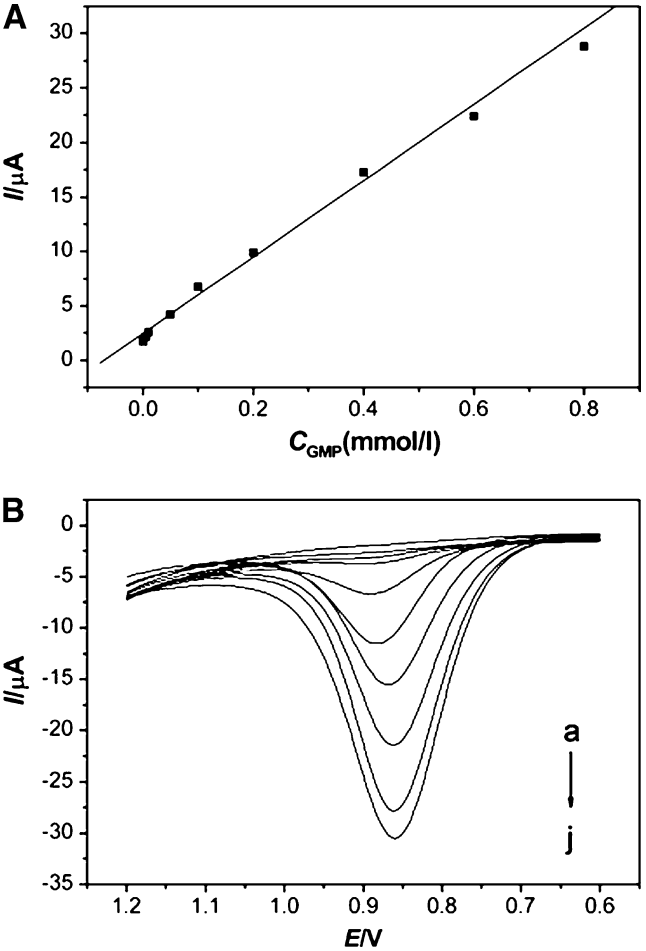

Fig. 9 **a** Differential Pulse Voltammetry of GMP at HTLC/GCE in acetate buffer solution with various concentrations (from a to f: 0, 1.0×10^{-6}, 5.0×10^{-6}, 1.0×10^{-5}, 5.0×10^{-5}, 1.0×10^{-4}, 2.0×10^{-4}, 4.0×10^{-4}, 6.0×10^{-4}, 8.0×10^{-4} molL^{-1}), scan rate: 100 mVs^{-1}, **b** The dependence of peak current on the concentration of GMP

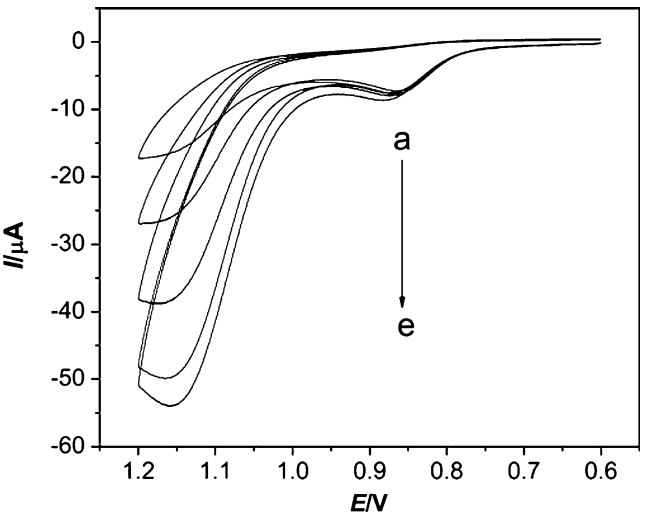

Fig. 10 Cyclic voltammograms of different GMP concentrations (from a to e: 1.0×10^{-4}, 2.0×10^{-4}, 4.0×10^{-4}, 6.0×10^{-4}, 8.0×10^{-4} molL^{-1}) in the presence of 2.0×10^{-4} molL^{-1} guanine (G) on the HTLC/GCE in pH 5.0 acetate buffer solution at the scan rate of 100 mVs^{-1}

carried out using DPV scanning (Fig. 8). From the oxidation peak current of guanine, guanosine and GMP, it could be seen the peak current of GMP was largest, followed by guanosine, and guanine was the minimum.

It is known that the N atom can be protonated to be positive in the weak acid environment. In the positive potential, guanine with positive charge is repelled by the modified electrode, so a small amount is adsorbed. While the guanosine's ribose in larger electronegativity can counteract the positive charged purine ring to be slightly negative, therefore, it has a higher adsorption than guanine in the electrode. However, it has an inferior adsorption than GMP in the electrode. Both the acid ribose ring and the phosphate anion in GMP have the negative charge which can be attracted by the surface positive charge of HTLC, so the GMP has the largest amounts on electrode surface. Guanine oxidation peak potential E_{pa} is about 0.80 V, guanosine and GMP oxidation potential are 1.04 and 1.08 V, respectively. The E_{pa} of three different substances indicates the reaction capacity of the purine ring is reduced due to the substitute of ribose ring and phosphate anion. Furthermore, guanosine and GMP have the similar response to E_{pa}, because the impact of phosphate radical to the guanine ring is smaller than acid ribose ring [42], as was shown in Fig. 8.

Calibration and limit of detection

Figure 9a displayed the DPV response of adsorbed GMP by SPE process at the HTLC modified GCE at various concentrations. The oxidation current was proportional to the concentration of GMP in the range of 1.0×10^{-6}–8.0×10^{-4} molL^{-1} (R=0.9945) (Fig. 9b), and the detection limit was estimated to be 5.0×10^{-7} molL^{-1} at a signal-to-noise ratio of 3, indicating an easy method to detect GMP was obtained. Hence, it can be concluded that the modified electrode HTLC/GCE shows excellent sensitivity and low detection limit for GMP.

Electrochemical response of GMP in the presence of guanine

Figure 10 showed the cyclic voltammograms of a mixed solution of containing 2.0×10^{-4} molL^{-1} guanine (G) with the changes concentrations of GMP from 1.0×10^{-4}–8.0×10^{-4} molL^{-1}. Two oxidation peaks appeared about at 0.860 and 1.160 V for G and GMP respectively, with the peak-to-peak separation as 300 mV, which was large enough to detect GMP in the G and GMP mixture solution. Thus, the HTLC modified electrode showed good ability to distinguish for the different electrochemical response.

Stability and reproducibility of the modified electrodes

The stability and reproducibility were evaluated by measuring the electrochemical response of 2.0×10^{-4} molL^{-1} GMP by HTLC/GCE. The modified electrode retained 93% of its initial response after it was kept in refrigerator at 4°C for 10 days, which indicated that the modified electrode had good stability. The reproducibility was investigated by five parallel modified electrodes. The relative standard deviation (RSD) was 5.90%, which suggested that the HTLC/GCE displayed a good reproducibility.

Conclusion

Cu-Mg-Al HTLC served as a selective sorbent, is able to extract GMP rapidly and effectively. Moreover, HTLC sorbent has some main advantages: thermal stability, chemical inertness, lack of toxicity, strong affinity for GMP. The electrochemical parameters of GMP on HTLC/GCE were carefully calculated with the electrochemical oxidation mechanism proposed. The result indicated that the positive charged Cu-Mg-Al hydrotalcite-like compound could provide a favorable microenvironment for GMP to realize the extractionon ability and the good promotion to the GMP oxidation. Moreover, the preparation of the sensor is simple and also has a lower cost. Hence, the HTLCs will be good modified electrode materials to detect biomolecules.

Acknowledgements This work was supported by the National Natural Science Foundation of China (No.20775044) and the Natural Science Foundation of Shandong province, China (Y2006B20).

References

1. Ciccarelli R, Ballerini P, Sabatino G, Rathbone MP, D'Onofrio M, Caciagli F, Di Iorio P (2001) Int J Dev Neurosci 19:395–414
2. Rathbone MP, Middlemiss PJ, Gysbergs JW, Andrew C, Herman MAR, Reed JK, Ciccarelli R, Iorio PD, Caciagli F (1999) Prog Neurobiol 59:663–690
3. Frizzo ME, Lara DR, Prokopiuk AS, Vargas CR, Salbego CG, Wajner M, Souza DO (2002) Cell Mol Neurobiol 22:353–363
4. Frizzo ME, Lara DR, Dahm KC, Prokopiuk AS, Swanson RA, Souza DO (2001) Neuro Report 12:879–881
5. Frizzo ME, Soares FA, Dall'Onder LP, Lara DR, Swanson RA, Souza DO (2003) Brain Res 972:84–89
6. Baron BM, Dudley MW, McCarty DR, Miller FP, Reynolds IJ, Schmidt CJ (1989) J Pharmacol Exp Ther 250:162–169
7. Lara DR, Schmidt AP, Frizzo ME, Burgos JS, Ramirez G, Souza DO (2001) Brain Res 912:176–180
8. Schmidt AP, Lara DR, Maraschin JF, Perla AS, Souza DO (2000) Brain Res 864:40–43

9. Vinade ER, Schmidt AP, Frizzo ME, Izquierdo I, Elisabetsky E, Souza DO (2003) Brain Res 977:97–102
10. Gänshirt KH, Krause J (1974) Dev Biol Standardization 27:123–128
11. Giannattasio S, Gagliardi S, Samaja M, Marra E (2003) Brain Res Protocols 10:168–174
12. Huang D, Zhang Y, Chen X (2003) J Chromatogr 784:101–109
13. Rajendra NG, Anuradha T (2005) Anal Bioanal Chem 382:1683–1690
14. Rajendra NG, Munetaka O, Anuradha T (2007) Anal Chimica Acta 581:32–36
15. Xie H, Yang D, Heller A, Gao Z (2007) Biophysical Journal 92:70–72
16. Liu Z, Ma R, Ebina Y, Iyi N, Takada K, Sasaki T (2007) Langmuir 23:861–867
17. Rives V, Ulibarri MA (1999) Coord Chem Rev 181:61–120
18. Scavetta E, Stipa S, Tonelli D (2007) Electrochem Commun 9:2838–3282
19. Ballarin B, Berrettoni M, Carpani I, Scavetta E, Tonelli D (2005) Anal Chim Acta 538:219–222
20. Guadggnini L, Ballarin B, Mignani A, Scavetta E, Tonelli D (2007) Sens Actuators B 126:492–498
21. Kaneda K, Ueno S, Imanaka T (1995) J Mol Catal A 102:135–138
22. Auer SM, Wandeler R, Göbel U, Baiker A (1997) J Catal 169:1–12
23. Velu S, Swamy CS (1996) Appl Catal A Gen 145:141–153
24. Shannon IJ, Rey F, Sankar G, Thomas JM, Maschmeyer T, Waller AM, Palomares AE, Corma A, Dent AJ, Greaves GN (1996) J Chem Soc 92:4331–4336
25. Li MG, Chen SH, Ni F, Wang YL, Wang L (2008) Electrochim Acta 53:7255–7260
26. Ai H, Huang X, Zhu Z, Liu J, Chi Q, Li Y, Li Z, Ji X (2008) Biosen Bioelectron 24:1048–1052
27. Rei MJ, Silvério F, Tronto J, Valim JB (2004) J Phys Chem Sol 65:487–492
28. Jitianu M, Bãlãsoiu M, Marchidan R, Zaharescu M, Crisan D, Craiu M (2000) Int J Inorg Mater 2:287–300
29. Hernandez Moreno MJ, Ulibarri MA, Rendon JL, Serna CJ (1985) Phys Chem Miner 12:34–38
30. Venugopal A, Palgunadi J, Deog JK, Joo OS, Shin CH (2009) Catal Today 147:94–99
31. Xu ZP, Xu R, Zeng HC (2001) Nano Lett 12:703–706
32. Kannan S, Dubey A, Knozinger H (2005) J Catal 231:381–392
33. Kishore D, Rodrigues A (2008) Appl Catal A Gen 345:104–111
34. Ballarin B, Gazzano M, Seeber R, Tonelli D, Vaccari A (1998) J Electroanal Chem 445:27–37
35. Carrero H, León LE (2001) Electrochem Commun 3:417–420
36. Zhang W, Yang T, Zhuang X, Guo Z, Jiao K (2009) Biosens Bioelectron 24:2417–2422
37. Laviron E (1974) J Electroanal Chem 52:355–393
38. Ferapontova EE (2004) Electrochim Acta 49:1751–1759
39. Goyal RN, Jain N, Garg DK (1997) Bioelectrochem Bioenerg 43:105–114
40. Adams RN (1969) Electrochemistry at solid electrodes. Marcel Dekker, New York
41. Anson FC (1964) Anal Chem 36:932–934
42. Shen H, Xia J, Su Z, Zhang Z (2001) J Chemical Chin Univer 22:962–965